A heat shock–responsive lncRNA *Heat* acts as a HSF1-directed transcriptional brake via m^{6}A modification

Quanquan Ji[a], Xin Zong[a,1], Yuanhui Mao[a], and Shu-Bing Qian[a,2]

[a]Division of Nutritional Sciences, Cornell University, Ithaca, NY 14853

Edited by Howard Y. Chang, Stanford University, Stanford, CA, and approved May 19, 2021 (received for review February 2, 2021)

Long noncoding RNAs (lncRNAs) are key regulators of gene expression in diverse cellular contexts and biological processes. Given the surprising range of shapes and sizes, how distinct lncRNAs achieve functional specificity remains incompletely understood. Here, we identified a heat shock–inducible lncRNA, *Heat*, in mouse cells that acts as a transcriptional brake to restrain stress gene expression. Functional characterization reveals that *Heat* directly binds to heat shock transcription factor 1 (HSF1), thereby targeting stress genes in a trans-acting manner. Intriguingly, *Heat* is heavily methylated in the form of m^{6}A. Although dispensable for HSF1 binding, *Heat* methylation is required for silencing stress genes to attenuate heat shock response. Consistently, m^{6}A depletion results in prolonged activation of stress genes. Furthermore, *Heat* mediates these effects via the nuclear m^{6}A reader YTHDC1, forming a transcriptional silencing complex for stress genes. Our study reveals a crucial role of nuclear epitranscriptome in the transcriptional regulation of heat shock response.

heat shock stress | long noncoding RNA | RNA modification

The evolutionarily conserved heat shock response (HSR) is essential for organismal survival upon proteotoxic stress (1). Initially discovered under thermal stress, HSR is orchestrated at multiple levels to ensure rapid and robust induction of cytoprotective genes encoding heat shock proteins (HSPs) (2, 3). In mammalian cells, the heat shock factor 1 (HSF1) is the master regulator of stress gene expression (4, 5). Under normal conditions, HSF1 is present in the cytoplasm as an inactive monomer. Upon heat stress, HSF1 is trimerized, phosphorylated, and translocated to the nucleus, where it binds to heat shock elements (HSEs) in promoters of HSP genes. A complete HSR comprises robust activation of stress genes followed by timely attenuation when the stress is eliminated. Whereas most studies focus on transcriptional activation of HSR, little is known about how stress genes are turned off during the recovery phase.

Recent efforts of large-scale transcriptome sequencing have documented a wide variety of long noncoding RNAs (lncRNAs) transcribed from eukaryotic genomes (6–8). Although a vast majority of lncRNAs reside within intergenic regions, some lncRNAs are transcribed from promoters and enhancers (9). For instance, promoter upstream transcripts (PROMPTs) are transcribed in the antisense direction by RNA polymerase II (Pol II) due to divergent transcription of active promoters (10). PROMPTs can reach approximately several kilobases upstream of the transcription start sites of protein-coding genes. Despite the increased lncRNA repertoire, the vast majority remains uncharacterized. Major challenges include identifying the regulatory targets of lncRNAs and understanding their biological functions. A growing amount of evidence indicates that lncRNAs regulate transcription via chromatin remodeling (11). Depending on the interacting factors, lncRNAs could act as activators or repressors of transcription. Some lncRNAs function only at their sites of synthesis to regulate local gene expression, whereas trans-acting lncRNAs diffuse from their site of synthesis and act on genes located at distant loci. The biochemical mechanisms of how differential lncRNAs target specific DNA regions with distinct consequences remain unclear.

One of the intriguing aspects of HSR is the heat-induced expression of lncRNAs (12). Upon heat stress, B2 RNA in mice and Alu RNA in humans are transcribed by RNA polymerase III (Pol III) from short interspersed elements (13). With little sequence homology, both lncRNAs function in trans as direct repressors of general Pol II activity, contributing to the inhibition of basal gene transcription following heat stress. Intriguingly, the polycomb protein EZH2 has been shown to cleave B2 RNA, resulting in transcriptional activation of stress genes (14). How up-regulation of stress genes is coordinated with down-regulation of housekeeping genes during HSR is currently not clear. In human cells, an interesting lncRNA termed HSR1 has been reported to act as an auxiliary factor of HSF1 activation (15), although its origin remains elusive. Despite our increasing understanding of HSR induction, whether lncRNAs play a role in HSR attenuation is currently unknown.

Notably, a large proportion of lncRNAs is subject to modifications in the form of N^6-methyladenosine (m^{6}A) (16). The nuclear m^{6}A signals have been shown to impact transcription. One well-characterized example is *Xist*, the lncRNA that mediates the transcriptional silencing of the entire X chromosome (17). The m^{6}A residues installed on *Xist* recruit the nuclear m^{6}A reader YTHDC1, forming a transcriptional silencing complex. A recent

Significance

The heat shock response is a universal homeostatic mechanism for cells to cope with adverse environmental conditions. However, little is known about whether an active mechanism is needed to turn off stress genes during stress recovery. We report a heat shock–inducible long noncoding RNA, *Heat*, in mouse cells that acts as a transcriptional brake to restrain stress gene expression during the recovery phase. We show that *Heat* targets specific stress genes via HSF1 as a carrier. Unexpectedly, *Heat* relies on m^{6}A modification and the m^{6}A reader YTHDC1 to silence stress genes to attenuate heat shock response. These results demonstrate an intimate connection between nuclear epitranscriptome and transcriptional regulation of heat shock response.

Author contributions: Q.J. and S.-B.Q. designed research; Q.J. and X.Z. performed research; Q.J., X.Z., Y.M., and S.-B.Q. analyzed data; and Q.J. and S.-B.Q. wrote the paper.

The authors declare no competing interest.

This article is a PNAS Direct Submission.

See online for related content such as Commentaries.

[1]Present address: College of Animal Sciences, Zhejiang University, Hangzhou 310058, People's Republic of China.

[2]To whom correspondence may be addressed. Email: sq38@cornell.edu.

This article contains supporting information online at https://www.pnas.org/lookup/suppl/doi:10.1073/pnas.2102175118/-/DCSupplemental.

Published June 15, 2021.

study reported that m^{6}A modification regulates the stability of chromatin-associated regulatory RNAs via YTHDC1, controlling the nearby chromatin state and transcription (18). Given the diversity and complexity of lncRNAs, whether m^{6}A relies on the unified mechanism for transcriptional regulation remains unknown.

In this study, we define a lncRNA *Heat* (heat-enhanced antisense transcript, also known as *Gm20005*) as an important transcriptional brake that attenuates HSR in mouse cells. Functional characterization reveals that *Heat* directly binds to HSF1 in vivo and in vitro, thereby targeting stress genes in a trans-acting manner. Intriguingly, *Heat* is heavily methylated in the form of m^{6}A. Although dispensable for HSF1 binding, this modification is required for silencing stress genes during recovery. Consistently, depletion of either m^{6}A or the m^{6}A reader YTHDC1 resulted in prolonged activation of stress genes. These results demonstrate an intimate connection between nuclear epitranscriptome and transcriptional regulation during HSR.

Results

Profiling of Chromatin-Associated RNAs Reveals Heat Shock–Induced lncRNAs. The transcriptional response of protein-coding genes during HSR has been extensively studied (19). To elucidate the role of noncoding RNAs in mammalian HSR, we investigated the landscape of chromatin-associated transcripts in mouse embryonic fibroblasts (MEFs) before and after heat shock stress. We modified native elongating transcript sequencing (20) by purifying chromatin-engaged RNA species followed by RNA-sequencing (chrRNA-seq) (Fig. 1*A* and *SI Appendix*, Fig. S1*A*). An oligo-dT purification step was omitted in order to capture partially synthesized and full-length RNA species. In parallel, total RNAs in the cytoplasm were collected and subjected to RNA-seq (cytRNA-seq). In agreement with the previous study (20), chrRNA showed a significantly lower exon/intron ratio than cytRNA (Fig. 1*B*), indicating that chromatin-associated transcripts are incompletely spliced. Interestingly, chrRNA derived from heat-stressed MEFs exhibited an increased exon/intron ratio relative to the unstressed control ($P < 2.2 \times 10^{-16}$) (Fig. 1*B*). The same feature can also be seen in published precision nuclear run-on sequencing (PRO-seq) data sets (19) (*SI Appendix*, Fig. S1*B*), excluding possible artifacts associated with chrRNA-seq. As illustrated for the housekeeping gene *Gapdh* (*SI Appendix*, Fig. S1*C*), introns are removed more efficiently from chrRNA after heat shock stress. We interpret the increased exon/intron ratio of chrRNA as a result of reduced transcriptional elongation under thermal stress, which promotes intron removal.

Since chrRNA contains nascent transcripts, the overall changes of gene expression upon heat stress are comparable between chrRNA and cytRNA (Fig. 1 *C* and *D*, Spearman's $Rho = 0.39$, $P < 2.2 \times 10^{-16}$). As expected, a vast majority of up-regulated genes are involved in protein folding and stress response (Fig. 1*C* and Dataset S1). Notably, not all the HSF1 target genes showed equal response to heat stress (Fig. 1*D*), which is in line with the broader role of HSF1 in organismal physiology (21). A subset of chrRNAs exhibited more evident increase than the cytRNA counterparts in stressed MEFs, suggesting the presence of heat shock–inducible

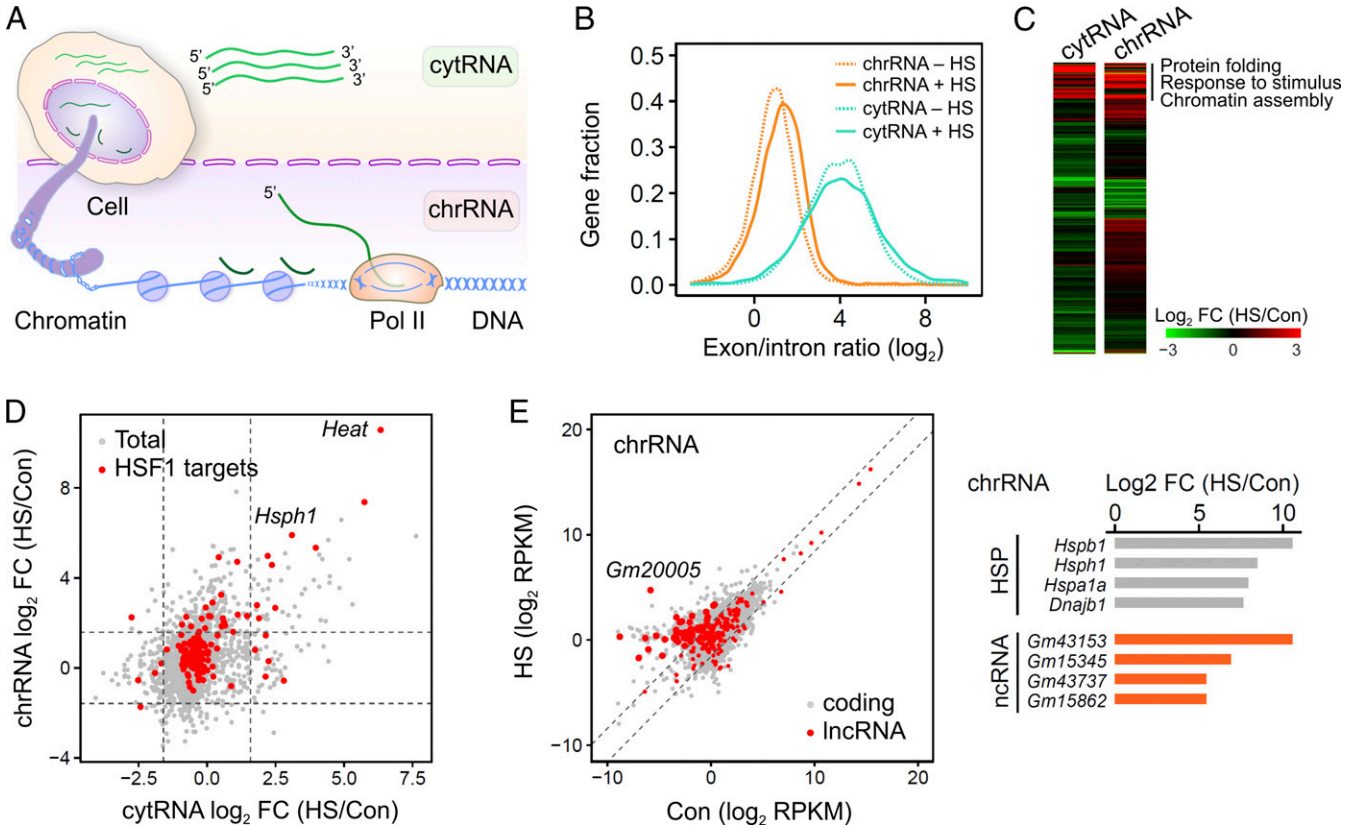

Fig. 1. Sequencing of chromatin-associated RNAs reveals heat shock–induced lncRNAs. (*A*) Schematic view of fractionated RNA species. CytRNA, cytosolic RNA; chrRNA, chromatin-associated RNA. (*B*) Distribution of exon/intron ratios of individual transcripts derived from cytRNA and chrRNA before and after heat shock stress (HS; 42 °C, 1 h; 37 °C, 3h). (*C*) A heatmap showing fold changes of cytRNA and chrRNA in response to heat shock stress. (*D*) A scatter plot showing the correlation of chrRNA changes to cytRNA changes in response to heat shock stress. Only genes detected in both cytRNA and chrRNA are shown. Genes targeted by HSF1 are highlighted in red. Dashed lines indicate the thresholds (fold change >3 or <1/3) for increased or reduced RNA levels. (*E*) A scatter plot showing the changes of chrRNA levels with or without heat shock stress. lncRNA are highlighted in red. Dashed lines indicate the thresholds (fold change >3 or <1/3) for increased or reduced chrRNA levels. *Right* shows the fold changes of the top four HSPs and top four lncRNAs in response to heat shock stress.

noncoding RNAs. Indeed, chrRNA-seq not only revealed up-regulated genes encoding HSPs but also uncovered several lncRNAs surged after heat stress (Fig. 1*E*). One lncRNA, *Gm20005*, showed a higher degree of increase (>1,500-fold) than *Hspa1a* in stressed MEFs.

Characterization of Heat Shock–Induced LncRNA *Gm20005* (*Heat*). We focused on *Gm20005* not only because of its being the most significantly induced lncRNA but also because it is located upstream of the stress gene *Hsph1* (encoding Hsp105) on chromosome 5 (Fig. 2*A*). Transcribed in the antisense orientation, *Gm20005* represents a PROMPT as a result of divergent transcription from the *Hsph1* promoter. We renamed this lncRNA as heat-enhanced antisense transcript (*Heat*), which has one isoform based on the genome annotation (*SI Appendix*, Fig. S2*A*). Using a series of oligos amplifying different exons, we confirmed the stress-induced up-regulation of *Heat* in MEF cells (*SI Appendix*, Fig. S2*B*). Using primers located at the 5′ and 3′ ends of *Heat*, we detected a transcript of 2,663 nucleotides containing two exons (*SI Appendix*, Fig. S2*A*). Notably, the kinetics of *Heat* expression resembles *Hsph1* (Fig. 2*B*), suggesting that both transcripts are transcribed by Pol II from the same promoter. Supporting this notion, α-amanitin treatment largely inhibited the induction of those transcripts upon heat stress. Remarkably, in an MEF cell line lacking HSF1, we observed little induction of stress genes including *Heat* (Fig. 2*C*). Therefore, in response to thermal stress, HSF1 not only activates stress genes but also triggers *Heat* expression via bidirectional transcription from the *Hsph1* promoter.

Like messenger RNAs (mRNAs), PROMPTs carry 5′ cap structures and 3′ polyadenosine tails. Using purified cap-binding protein eIF4E, we confirmed that *Heat* is capped with m^7G (Fig. 2*D*). Additionally, oligo d(T) readily pull down *Heat* with a similar efficiency as *Hsph1* but not 18S ribosomal RNA (Fig. 2*E*). Although PROMPTs are believed to be short lived, we found that the half-life of *Heat* is similar to mRNAs like *Hsph1* (*SI Appendix*, Fig. S2*C*). To characterize the translational potential of *Heat*, we conducted polysome profiling of stressed MEFs using sucrose gradient. Unlike *Hspa1a* that encodes Hsp70, *Heat* was barely recovered from the polysome (*SI Appendix*, Fig. S2*D*). Further supporting the noncoding feature of *Heat*, >95% of *Heat* RNA was present in the chromatin fraction of MEFs after heat stress

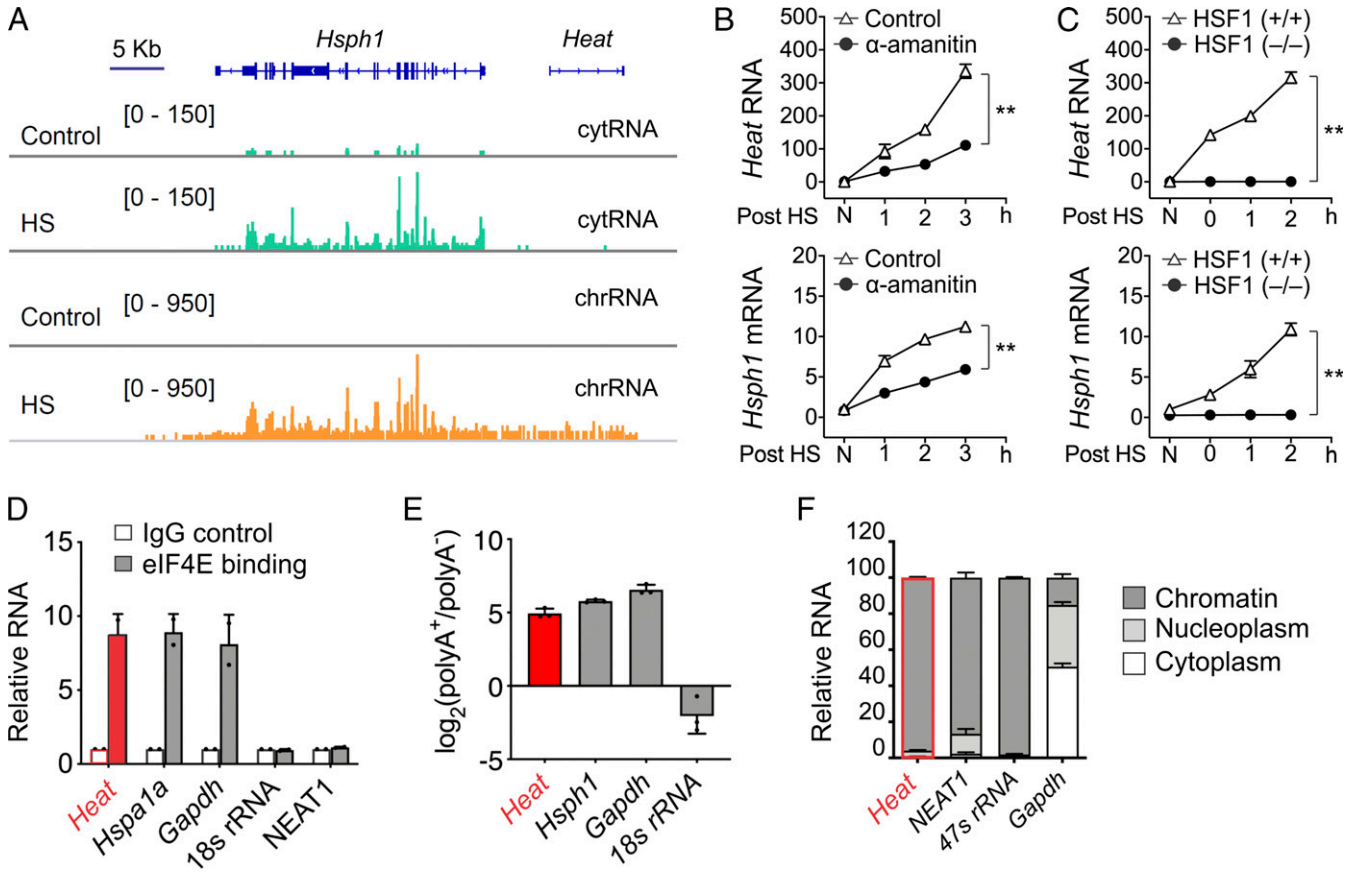

Fig. 2. Characterize heat shock–induced LncRNA *Gm20005* (*heat*). (*A*) *Top*, schematic illustration of genomic loci of *Heat* and *Hsph1* on mouse chromosome 5. A representative genomic region covering the *Hsph1* and *Heat* locus shows the read density of cytRNA (*Middle*, light green) and chrRNA (*Bottom*, light orange) in MEFs before (control) and after (HS; 42 °C, 1 h; 37 °C, 3 h) heat shock stress. (*B*) MEFs were subject to heat shock stress (42 °C, 1 h) followed by recovery at 37 °C for various times in the absence or presence of α-amanitin (0.25 mM). N, no heat shock. Total *Heat* (*Top*) and *Hsph1* (*Bottom*) RNA levels were quantified by RT-qPCR. Error bars, mean ± SEM; $^{**}P < 0.01$; $n = 3$, biological replicates. (*C*) MEF cells with ($HSF1^{+/+}$) or without ($HSF1^{-/-}$) HSF1 were subject to heat shock stress (42 °C, 1 h) followed by recovery at 37 °C for various times. N, no heat shock. Total *Heat* (*Top*) and *Hsph1* (*Bottom*) RNA levels were quantified by RT-qPCR. Error bars, mean ± SEM; $^{**}P < 0.01$; $n = 3$, biological replicates. (*D*) Purified GST-eIF4E protein was incubated with cell lysates derived from heat-stressed MEF cells (42 °C, 1 h; 37 °C, 1 h). The eIF4E bound RNA was extracted followed by RT-qPCR analysis. Error bars, mean ± SEM; $n = 3$, biological replicates. (*E*) Total RNA extracted from heat-stressed MEF cells (42 °C 1 h, 37 °C 1 h) was incubated with Dynabeads $Oligo(dT)_{25}$. Beads bound ($polyA^+$) and unbound RNA ($polyA^-$) was extracted followed by RT-qPCR analysis. Error bars, mean ± SEM; $n = 3$, biological replicates. (*F*) Cell fractionation was followed by RT-qPCR to detect the distribution of indicated transcripts in heat-stressed MEF cells. The RT-qPCR data represented a percentage of the total amount of detected transcripts. Error bars, mean ± SEM; $n = 3$, biological replicates.

(Fig. 2*F*). Collectively, *Heat* is a heat shock–inducible PROMPT derived from the *Hsph1* promoter.

Depletion of *Heat* from MEFs Enhances HSR. To elucidate the biological role of *Heat*, we designed antisense oligonucleotides (ASOs) containing locked nucleic acids to target nuclear *Heat* for degradation by RNase H. We were able to achieve a >75% decrease of *Heat* levels in stressed MEFs after ASO transfection (Fig. 3*A*). Compared to the cells treated with control ASO, *Heat* depletion significantly increased the heat stress–induced *Hsph1* expression (Fig. 3*B*). Remarkably, this effect is not limited to the local region. We observed a further up-regulation of *Hspa1a* in the absence of *Heat* (Fig. 3*B*). By contrast, no effect was observed for housekeeping genes like *Actb*. The negative regulation of stress genes by *Heat* was further manifested by increased Hsp70 protein levels in the heat-stressed MEFs lacking *Heat* (Fig. 3*C*). The same finding holds true by *Heat* knockdown using short hairpin RNAs (shRNAs) (*SI Appendix*, Fig. S3 *A* and *B*). This was not due to the stabilization of stress mRNAs because both *Hsph1* and *Hspa1a* exhibited similar turnover before and after *Heat* silencing (*SI Appendix*, Fig. S3*C*). To confirm that the up-regulation occurs at the transcription level, we measured nascent mRNA levels in stressed cells by 4-thiouridine (s4U) labeling followed by biotinylation. *Heat* knockdown led to approximate threefold increase of nascent *Hsph1* and *Hspa1a* levels after heat stress (Fig. 3*D*). Since the housekeeping gene *Actb* showed little difference, it appears that *Heat* acts as a repressor of stress genes during HSR. Given the distal effect of *Heat* on the transcription of stress genes, we next examined whether an ectopic plasmid encoding the firefly luciferase (Fluc) reporter is subjected to regulation by *Heat*. Indeed, *Heat* silencing resulted in a marked increase (>fourfold) of Fluc levels driven by the *Hspa1a* promoter but not the *Actb* promoter (Fig. 3*E*). Taken together, the stress-inducible *Heat* acts as a trans-acting repressor to attenuate HSR, forming a negative feedback loop.

***Heat* Acts on HSF1 via Direct Binding.** To understand how *Heat* regulates HSR, we conducted chromatin immunoprecipitation (ChIP) assays using HSF1-specific antibodies. As expected, in control cells, binding of HSF1 to the *Hspa1a* promoter occurred rapidly upon heat stress at 42 °C and began to decline when the temperature was back to 37 °C (Fig. 4*A*). However, in MEF cells lacking *Heat*, the same stress resulted in about twofold as much HSF1 associated with the promoter. Interestingly, *Heat* does not seem to affect HSF1 activation because its phosphorylation status remained comparable in cells with or without *Heat* silencing (Fig. 4*B*). Since *Heat* acts on HSF1 targeted genes, it is possible that *Heat* directly binds to HSF1. To test this possibility, we enriched HSF1-associated RNAs by zero-distance cross-linking followed by RT-qPCR. HSF1 coprecipitated more *Heat* (~12-fold) than the negative control *Gapdh* mRNA (Fig. 4*C*). To substantiate this finding further, we transfected MEF cells with HSF1 fused with APEX2, an ascorbate peroxidase that enables proximity-dependent biotin labeling (22) (*SI Appendix*, Fig. S4 *A* and *B*). APEX2-HSF1 readily biotinylated *Heat* but not *Gapdh* from stressed MEF cells (*SI Appendix*, Fig. S4*C*).

To demonstrate the binding kinetics between *Heat* and HSF1, we conducted the electrophoretic mobility shift assay (EMSA) using *Heat* synthesized via in vitro transcription and recombinant HSF1 purified from *Escherichia coli*. Compared to the synthesized HSE DNA fragments that showed an expected strong affinity to HSF1 (K_d = 0.475 μM), *Heat* exhibited a lower binding affinity (K_d = 3.493 μM) (Fig. 4*D*). Therefore, it is unlikely that *Heat* competes with HSE for HSF1 binding. Intriguingly, a competition assay revealed altered migration of HSE–HSF1 complexes in the presence of *Heat* (Fig. 4*E*), suggesting the formation of *Heat*–HSE–HSF1

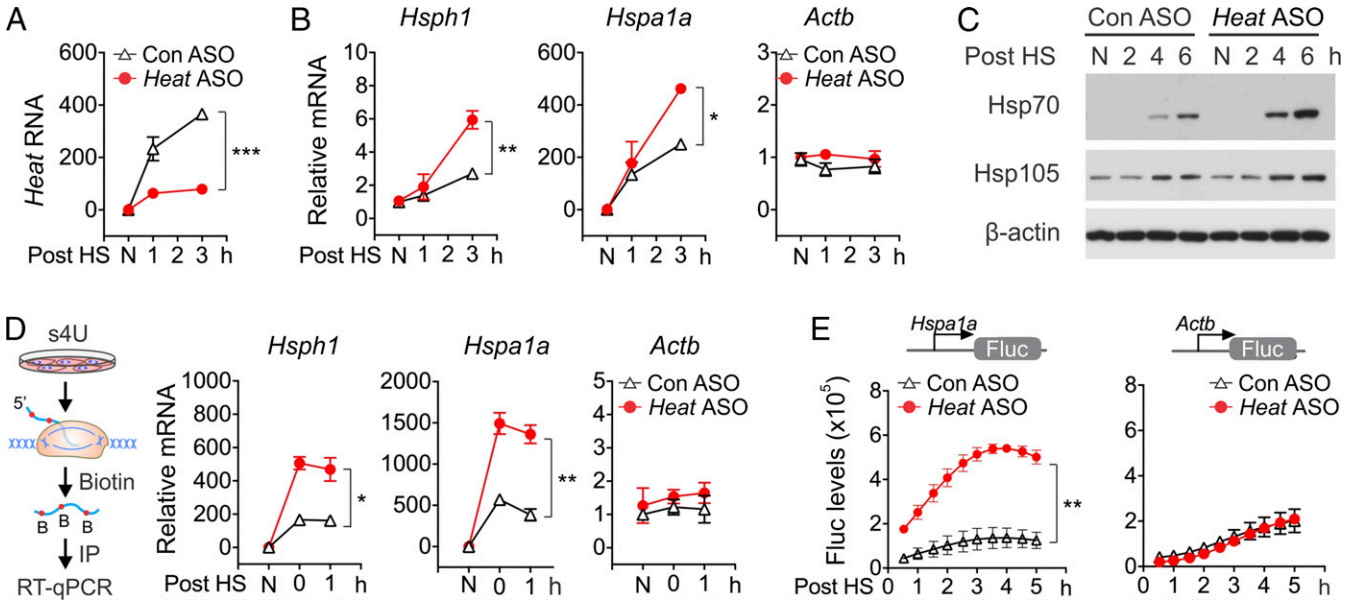

Fig. 3. Depletion of *heat* from MEFs enhances HSR. (*A*) MEF cells with (*Heat* ASO) or without (Control ASO) *Heat* knockdown were subject to heat shock stress (42 °C, 1 h) followed by recovery at 37 °C for various times. N, no heat shock. Total RNA was extracted followed by RT-qPCR analysis. Error bars, mean ± SEM; ***$P < 0.001$; $n = 3$, biological replicates. (*B*) RT-qPCR quantifies *Hsph1*, *Hspa1a*, and *Actb* from the same samples of *A*. Error bars, mean ± SEM; *$P < 0.05$, **$P < 0.01$; $n = 3$, biological replicates. (*C*) MEF cells with or without *Heat* knockdown were subject to heat shock stress (42 °C, 1 h) followed by recovery at 37 °C for various times. N, no heat shock. Whole-cell lysates were immunoblotted using antibodies indicated. (*D*) MEF cells with or without *Heat* knockdown were subject to heat shock stress (42 °C, 1 h) followed by recovery at 37 °C for various times. N, no heat shock. Nascent RNAs pulsed with 1 mM 4-thiouridine (s4U) were purified and followed by RT-qPCR analysis. Data were normalized to s4U-labeled spike in RNA. Error bars, mean ± SEM; *$P < 0.05$, **$P < 0.01$; $n = 3$, biological replicates. (*E*) MEF cells with or without *Heat* knockdown were transfected with plasmids encoding a Fluc reporter driven by either *Hspa1a* or *Actb* promoter. Transfected cells were subject to heat shock stress (42 °C, 1 h) followed by recovery at 37 °C for various times. Fluc activities were determined by luminometry. Error bars, mean ± SEM; **$P < 0.01$; $n = 3$, biological replicates.

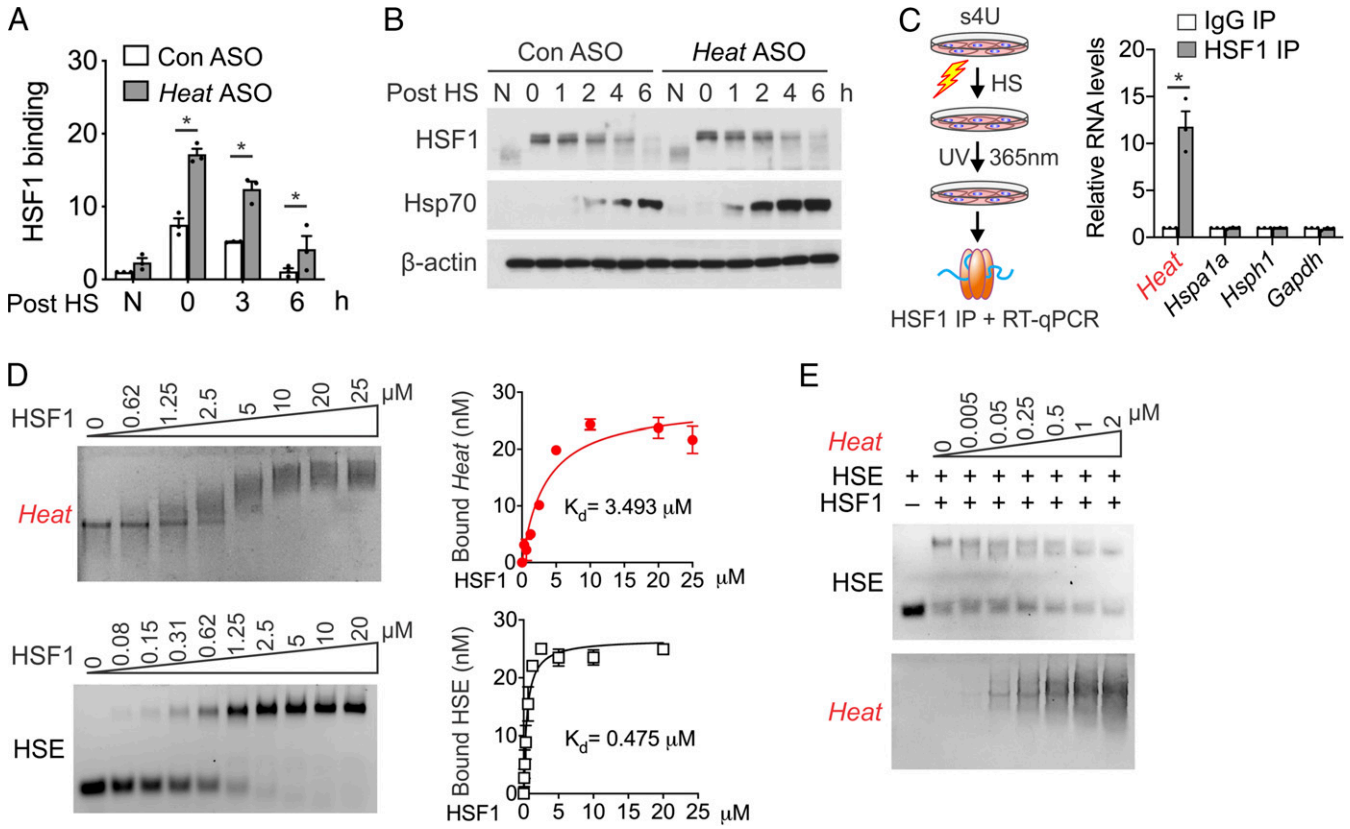

Fig. 4. *Heat* acts on HSF1 via direct binding. (*A*) MEF cells with (*Heat* ASO) or without (Con ASO) *Heat* knockdown were subject to heat shock stress (42 °C 1 h) followed by recovery at 37 °C for various times. ChIP analysis was performed using HSF1 antibody and followed by RT-qPCR analysis targeting the *Hspa1a* promoter. Error bars, mean ± SEM; **P* < 0.05; *n* = 3, biological replicates. (*B*) MEF cells with or without *Heat* knockdown were subject to heat shock stress (42 °C, 1 h) followed by recovery at 37 °C for various times. Whole-cell lysates were used for immunoblotting using antibodies indicated. The differential migration of HSF1 indicates the phosphorylation status. N, no heat shock. Whole-cell lysates were immunoblotted using antibodies indicated. (*C*, *Left*) Schematic of zero-distance cross-linking methodology. s4U-labeled RNAs were cross-linked to directly associated proteins using 365 nm ultraviolet light (UV). HSF1-associated RNA were purified followed by RT-qPCR analysis. (*Right*) RT-qPCR analysis of HSF1 immunoprecipitated RNAs (HSF1 IP) compared to IgG immunoprecipitated RNAs (IgG IP). Error bars, mean ± SEM; **P* < 0.05; *n* = 3, biological replicates. (*D*, *Left*) EMSA shows HSF1 binds *Heat* directly. Increasing concentration of recombinant HSF1 was incubated with 25 nM *Heat* or FAM-labeled double stranded DNA probes containing HSE. (*Right*) K_d values were calculated by saturation binding curves. Error bars, mean ± SEM; *n* = 3, biological replicates. (*E*) Recombinant HSF1 (0.1 μM) was preincubated with 5 nM HSE before various concentration of *Heat* was added. Signals from FAM-labeled HSE were recorded using a ChemiDoc imaging system (Bio-Rad). Gel was then stained with ethidium bromide to show the position of *Heat*.

supercomplexes. We hypothesize that *Heat* uses HSF1 as a carrier to target stress genes but relies on other mechanisms to suppress transcription.

***Heat* Represses Transcription in an m^{6}A-Dependent Manner.** Many lncRNAs have been demonstrated to regulate gene expression via chromatin interaction (23). We next examined whether the forced presence of *Heat* on the promoter of housekeeping genes would have similar effects as on stress genes. To address this question, we employed CRISPR-Display to deploy *Heat* to different genomic loci (Fig. 5*A*). MEF cells were cotransfected with plasmids encoding dCas9 and *Heat* fused to single guide RNA (sgRNA) targeting either *Hspa1a* or *Gapdh* promoters. Nascent RNA measurement revealed that *Gapdh*-localized *Heat* exhibited little effects on gene transcription. Only *Heat* targeting *Hspa1a* reduced the expression *Hspa1a* in heat-stressed cells (Fig. 5*A*). The negligible effect of *Heat* on *Gapdh* transcription further supports the notion that *Heat* relies on HSF1 to attenuate stress gene expression.

As an independent validation, we repeated this experiment using *Heat* RNA and sgRNAs synthesized in vitro. To our surprise, RNA transfection resulted in modest effects on *Hspa1a* expression (Fig. 5*B*). One of the key differences between plasmid and RNA transfection is that RNA molecules transcribed inside cells are subject to chemical modifications. In particular, RNA modification in the form of m^{6}A primarily occurs in a cotranscriptional manner (24). Intriguingly, *Heat* contains multiple m^{6}A sites with the consensus sequence motif RRACH (in which R represents A or G, and H represents A, C, or U). We conducted m^{6}A-seq of chrRNAs and confirmed at least eight methylation sites on *Heat* (*SI Appendix*, Fig. S5*A*), which was verified by RT-qPCR of m^{6}A-enriched fragments using individual oligos (*SI Appendix*, Fig. S5*B*). Remarkably, when randomly methylated *Heat* was synthesized and delivered into cells, we observed a significant repression of heat stress–induced gene expression like *Hspa1a* and *Hsph1* (Fig. 5*B*). The differential effect of methylated and nonmethylated *Heat* was particularly evident on heat stress–induced Hsp70 protein levels (Fig. 5*C*). It appears that *Heat* represses stress gene expression in a m^{6}A-dependent manner.

METTL3 Mediates Transcriptional Attenuation of Stress Genes. Many nascent RNAs are subject to m^{6}A installation in a cotranscriptional manner by METTL3, the core methyltransferase of m^{6}A (24). An in vitro methylation assay confirms METTL3/14-mediated *Heat* methylation, even in the absence of HSF1 (*SI Appendix*, Fig. S5*C*). To examine the role of m^{6}A in *Heat*-mediated stress gene silencing, we established an MEF cell line lacking

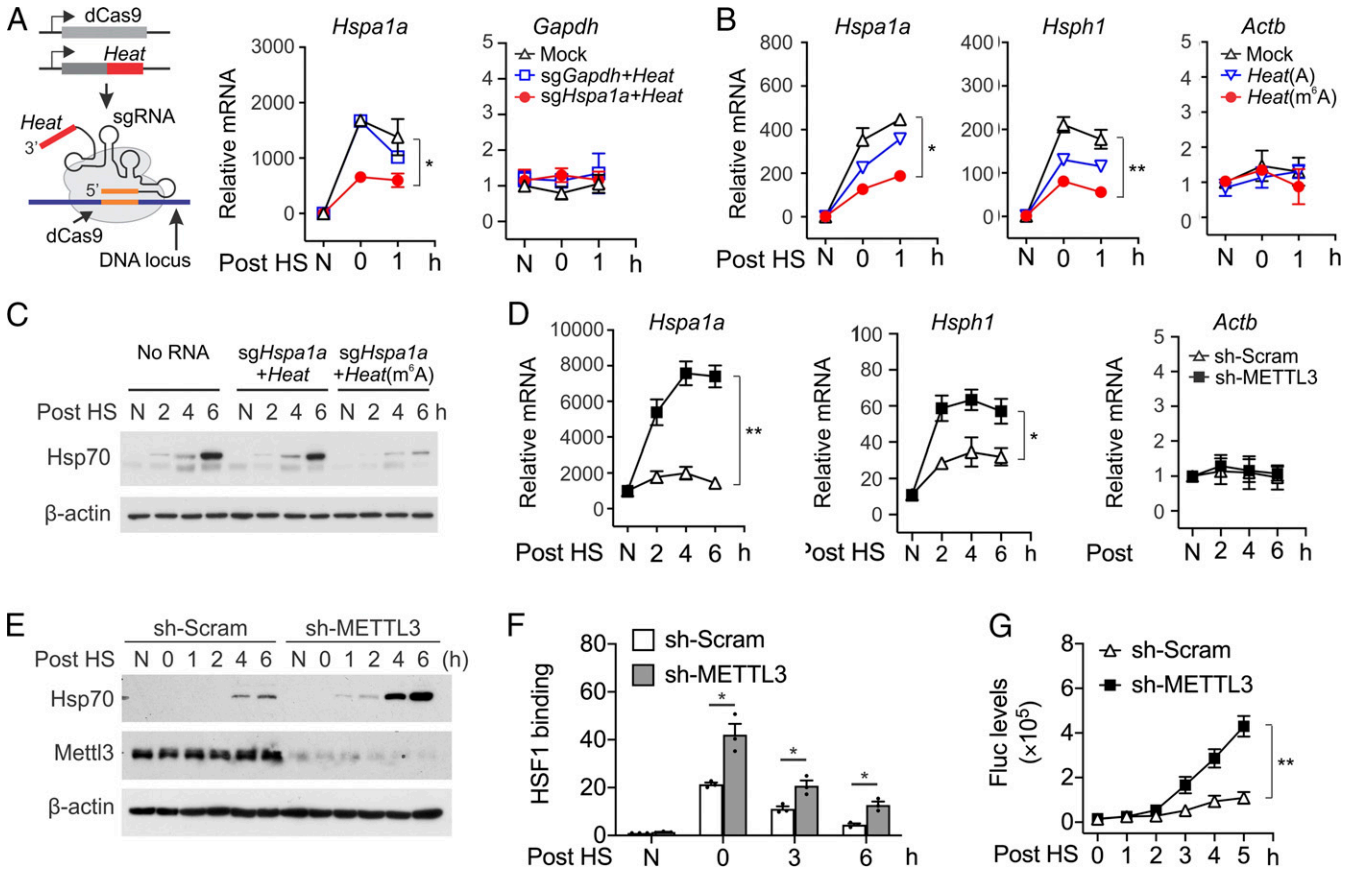

Fig. 5. *Heat* represses transcription in a m^{6}A-dependent manner. (*A*, *Left*) Schematic illustration of CRISPR-Display system: *Heat* is targeted to a specific DNA locus via sgRNA sequences and dCas9 protein. (*Right*) *Heat* was targeted to either *Hspa1a* gene locus (sg*Hspa1a* + *Heat*) or *Gapdh* gene locus (sg*Gapdh* + *Heat*) in MEF cells. After 1 h heat stress and various times of recovery, nascent RNA was pulsed with s4U, captured, and followed by RT-qPCR analysis. Error bars, mean ± SEM; $*P < 0.05$; $n = 3$, biological replicates. (*B*) In vitro transcribed *Heat* with or without m^{6}A modification was targeted to *Hspa1a* gene locus in MEF cells. After 1 h heat stress and various times of recovery, nascent RNA was pulsed with s4U, captured, and followed by RT-qPCR analysis. Error bars, mean ± SEM; $*P < 0.05$, $**P < 0.01$; $n = 3$, biological replicates. (*C*) Whole-cell lysates from the same sample as *B* were immunoblotted using antibodies indicated. (*D*) MEF cells with or without METTL3 knockdown were subject to heat shock stress (42 °C, 1 h) followed by recovery at 37 °C for various times. N, no heat shock. Total RNA was extracted followed by RT-qPCR analysis. Error bars, mean ± SEM; $*P < 0.05$, $**P < 0.01$; $n = 3$, biological replicates. (*E*) Whole-cell lysates from the same sample as *D* were immunoblotted using antibodies indicated. (*F*) MEF cells with or without METTL3 knockdown were subject to heat shock stress (42 °C, 1 h) followed by recovery at 37 °C for various times. ChIP analysis was performed using an HSF1 antibody and followed by RT-qPCR analysis targeting the *Hspa1a* promoter. Error bars, mean ± SEM; $*P < 0.05$; $n = 3$, biological replicates. (*G*) MEF cells with or without METTL3 knockdown were transfected with plasmids encoding a Fluc reporter driven by the *Hspa1a* promoter. Transfected cells were subject to heat shock stress (42 °C, 1 h) followed by recovery at 37 °C for various times. Fluc activities were determined by luminometry. Error bars, mean ± SEM; $**P < 0.01$; $n = 3$, biological replicates.

METTL3. METTL3 knockdown reduces m^{6}A levels across chrRNAs, including *Heat* (*SI Appendix*, Fig. S5*D*). Upon heat shock stress, the majority of stress genes showed higher induction in the absence of METTL3 as evidenced by cytRNA-seq and chrRNA-seq (*SI Appendix*, Fig. S5*E*). RT-qPCR validated the enhanced stress gene induction as exemplified by *Hspa1a* and *Hsph1* (Fig. 5*D*). As a result, the induction of Hsp70 was markedly enhanced in the absence of METTL3 (Fig. 5*E*). A similar observation was seen in MEFs lacking METTL14 (*SI Appendix*, Fig. S5 *F* and *G*). Direct measurement of *Hspa1a* turnover revealed little difference in cells with or without METTL3 knockdown (*SI Appendix*, Fig. S5*H*), thereby excluding the possibility that the increased stress mRNA abundancy is due to impaired turnover. Further supporting the crucial role of m^{6}A in the transcription of stress genes, ChIP assays revealed increased HSF1 binding to the *Hspa1a* promoter in MEFs lacking METTL3 (Fig. 5*F*). Additionally, METTL3 knockdown also enhanced Fluc levels driven by the *Hspa1a* promoter (Fig. 5*G*). These results support the crucial role of m^{6}A in *Heat*-mediated stress gene silencing.

YTHDC1 Mediates Transcriptional Attenuation of Stress Genes. m^{6}A could affect RNA secondary structures, thereby influencing the interaction of RNA-binding proteins. However, EMSA assays of HSF1 revealed comparable binding affinities between methylated and nonmethylated *Heat* (*SI Appendix*, Fig. S6*A*). Alternatively, m^{6}A executes its functionality via "reader" proteins such as YTH proteins. A recent study reported that methylation of chromatin-associated RNAs regulates transcription via YTHDC1, a nuclear m^{6}A reader (18). Indeed, IP of endogenous YTHDC1 readily pull down *Heat* from stressed MEFs (Fig. 6*A*). Like METTL3 silencing, knocking down YTHDC1 from MEFs resulted in an up-regulation of stress genes such as *Hspa1a* in response to heat stress as evidenced by nascent RNA measurement (Fig. 6*B*) and immunoblotting (Fig. 6*C*). Once again, YTHDC1 depletion did not affect the stability of *Heat* and *Hspa1a* (*SI Appendix*, Fig. S6*B*).

The nuclear m^{6}A reader YTHDC1 has been shown to regulate nuclear export of methylated mRNAs (25). However, many stress-responsive transcripts are capable of escaping the nuclear export quality control (26). Indeed, silencing YTHDC1 did not affect the cytosol/nuclear ratio for both *Hspa1a* and *Hsph1* mRNAs, albeit their steady-state levels were increased (*SI Appendix*, Fig. S6*C*). A

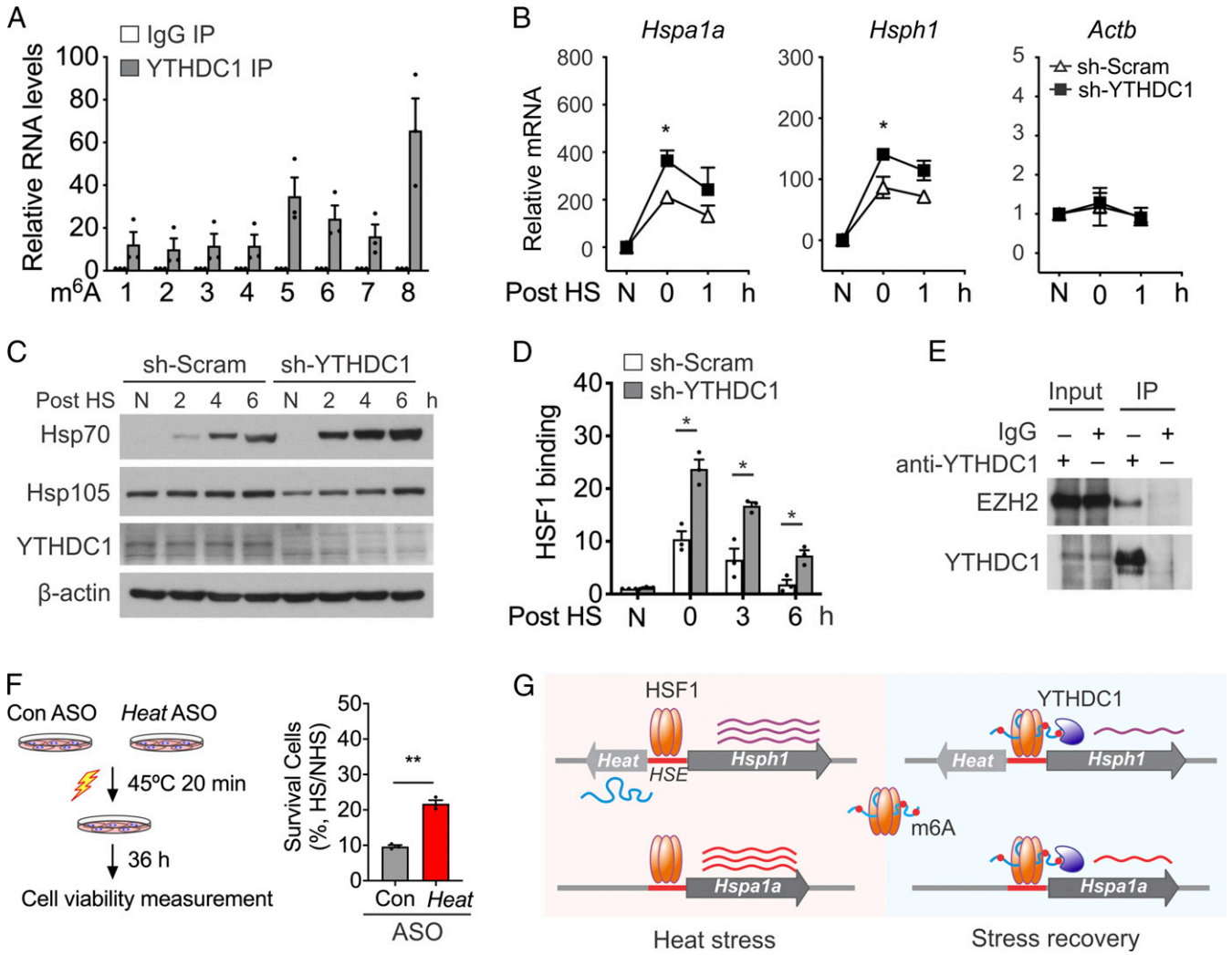

Fig. 6. YTHDC1 mediates transcriptional attenuation of stress genes. (*A*) YTHDC1-enriched *Heat* were analyzed by RT-qPCR. Regions detected by qPCR primers are shown in *SI Appendix*, Fig. S5*A*. Error bars, mean ± SEM; $n = 3$, biological replicates. (*B*) MEF cells with or without YTHDC1 knockdown were subject to heat shock stress (42 °C, 1 h) followed by recovery at 37 °C for various times. N, no heat shock. Nascent RNA was pulsed with s4U, captured, and followed by RT-qPCR analysis. Error bars, mean ± SEM; $^*P < 0.05$; $n = 3$, biological replicates. (*C*) MEF cells with or without YTHDC1 knockdown were subject to heat shock stress (42 °C, 1 h) followed by recovery at 37 °C for various times. N: no heat shock. Whole-cell lysates were immunoblotted using antibodies indicated. (*D*) MEF cells with or without YTHDC1 knockdown were subject to heat shock stress (42 °C, 1 h) followed by recovery at 37 °C for various times. ChIP analysis was performed using an HSF1 antibody and followed by RT-qPCR analysis. Error bars, mean ± SEM; $^*P < 0.05$; $n = 3$, biological replicates. (*E*) Whole-cell lysates from MEF cells were immunoprecipitated by anti-YTHDC1 antibodies followed by immunoblotting using antibodies as indicated. (*F*) MEF cells with or without *Heat* knockdown were subject to heat shock stress (45 °C, 20 min) followed by recovery at 37 °C for 36 h. Cell viability was measured by cell counting. Error bars, mean ± SEM; $^{**}P < 0.01$; $n = 3$, biological replicates. (*G*) A proposed model for *Heat*-mediated attenuation of HSR. In response to heat shock stress, activated HSF1 not only induces *Hsph1* but also triggers expression of a lncRNA *Heat* from the same promoter. *Heat* is heavily methylated in the form of m^6A and targets stress genes by directly binding to HSF1. The m^6A mark recruits YTHDC1 and forms a transcriptional silencing complex, thereby attenuating stress gene expression during stress recovery.

previous study reported that YTHDC1 also regulates mRNA splicing (27). Since *Hspa1a* is intronless, we focused on *Hsph1* and found that YTHDC1 knockdown led to an increased exon skipping for at least one exon (*SI Appendix*, Fig. S6*D*). The finding potentially explains the discrepancy between *Hsph1* mRNA and protein levels in the absence of YTHDC1 (Fig. 6*C*). Nevertheless, it is clear that YTHDC1 knockdown increases stress gene expression. Supporting this notion, silencing YTHDC1 enhanced HSF1 binding to the *Hspa1a* promoter (Fig. 6*D*), a strong indication of transcriptional up-regulation.

YTHDC1 has been shown to recruit regulatory components to silence X chromosome (17). In particular, analysis of the YTHDC1 interaction database identified components of the polycomb repressive complex 1 (PRC1) and 2 (PRC2) (28). Indeed, endogenous YTHDC1 readily pull down the EZH2 subunit of PRC2 (Fig. 6*E*). We conclude that *Heat* relies on YTHDC1 to form a silencing complex, thereby attenuating stress gene expression. Given the prolonged stress gene induction in cells lacking *Heat*, we reasoned that those cells would be more resistant to heat stress. This was indeed the case. Upon exposure to severe heat stress (45 °C), more cells were survived in the absence of *Heat* (Fig. 6*F*).

Discussion

One of the most amazing aspects of HSR is its complex, dynamic, and temporal regulation at both transcriptional and translational levels (1). Numerous factors act as transcriptional and post-transcriptional checkpoints to ensure that the magnitude and duration of HSR is rigorously controlled. Since prolonged HSR

is detrimental to cell physiology (29), cells also need to turn off HSR in a timely manner (30). By focusing on the transcription factor HSF1, enormous progress has been made in delineating how this transcriptional program is induced and attenuated (4). Mammalian genomes also encode regulatory RNAs that control gene expression during development and stress response (6, 8). While the role of microRNAs in these processes is well established, how lncRNAs influence HSR is still poorly understood.

In this study, we demonstrate that a PROMPT from *Hsph1* locus, *Heat*, contributes to the attenuation of stress gene expression in mouse cells (Fig. 6*G*). Unlike lncRNAs emerging from repetitive genomic regions, *Heat* is induced by HSF1 and transcribed by Pol II. Despite the presence of a 5′ cap and 3′ poly(A) tail, *Heat* is not actively translated presumably due to its nuclear localization. Functional characterization of *Heat* clearly suggests its role as a transcriptional brake to restrain stress gene expression. Using both loss-of-function and gain-of-function approaches, we have obtained critical insights into the biological functions of *Heat*. Depletion of stress-induced *Heat* resulted in an augmented stress gene expression, which was not limited to the neighboring protein-coding gene *Hsph1*. The apparent trans-acting feature of *Heat* is interesting. The mechanism whereby many lncRNAs specially localize to their target genomic loci to regulate gene expression remains poorly understood. Some lncRNAs, such as *NEAT1* and *MALAT1*, interact with nascent pre-mRNAs at specific genomic loci (31). The lncRNAs like *PARTICLE* and *MEG3* target DNA sequences by forming higher-order DNA–RNA triplex structures (32, 33). Instead of relying on specific base pairing with either DNA or mRNA, *Heat* uses HSF1 as a carrier by forming a ribonucleoprotein complex. Supporting this model, forced presence of *Heat* at nonstress genes by CRISPR-Display did not repress the targeted gene expression. This finding implies that *Heat* is not only induced by HSF1 but also relies on HSF1 for its functionality, forming a self-regulatory mechanism to fine-tune HSR.

Notably, the promoter of human *HSPH1* also undergoes divergent transcription as evidenced by PRO-seq (34). However, the promoter upstream noncoding RNA (annotated as *LOC105370148*) has no sequence homology compared to the mouse *Heat* (*SI Appendix*, Fig. S7*A*). Although *LOC105370148* was up-regulated in response to heat shock stress (*SI Appendix*, Fig. S7*B*), silencing *LOC105370148* using ASO did not seem to enhance *HSPA1A* expression (*SI Appendix*, Fig. S7*C*). The lack of human *HEAT* could potentially explain the differential basal levels of HSPs between human and rodent cells. We cannot exclude the possibility that some not-yet-identified lncRNAs may act like *Heat* in attenuating HSR in human cells.

In addition to identifying physiologic functions for *Heat*, we provide mechanistic insights into how *Heat* controls stress gene expression. Although many lncRNAs influence transcription by affecting chromatin accessibility, *Heat* relies on the m^{6}A mark to silence target genes. This mechanism is reminiscent of *XIST*-mediated gene silencing, which involves m^{6}A modification and the nuclear m^{6}A reader protein YTHDC1 (17). Indeed, knocking out either the methyltransferase METTL3 or YTHDC1 resulted in enhanced stress gene expression after heat shock, resembling *Heat* depletion. These results provide compelling evidence for the functional connection between *Heat* and m^{6}A. Given the pleiotropic effects of m^{6}A (16), we cannot be certain that all of these effects are due to the loss of *Heat* function. A recent study reported that the transcription activation induced by m^{6}A depletion is coupled with the accumulation of chromatin-associated regulatory RNAs (18). However, this mechanism does not explain the action of lncRNAs that negatively regulate gene transcription. Our study lends further credence to the idea that the m^{6}A mark could regulate gene expression in a highly specific manner by coordinating distinct lncRNAs. For lncRNAs like *Heat*, the installed m^{6}A does not promote RNA decay but rather recruits additional regulators via YTHDC1. Notably, the divergent effects of m^{6}A on transcriptional and translational regulation of stress gene expression is compatible with the unique timing of HSR. Upon heat stress, the increased 5′untranslated region (5'UTR) methylation facilitates cap-independent translation of stress proteins in the cytosol (35). During recovery, the excess m^{6}A signal in the nucleus turns off stress gene expression in a timely manner. Coordination of spatial and temporal regulation of gene expression ensures that the magnitude and duration of HSR are rigorously controlled. Therefore, nascent RNA modification acts as an important component of the molecular circuitry to prevent constitutive activation of stress genes.

In summary, we have employed detailed molecular and genetic approaches to demonstrate that the heat stress–induced lncRNA *Heat* contributes to the attenuation of HSR via direct HSF1 interaction. The functional connection between *Heat* and m^{6}A acts as an important component of the molecular circuitry to prevent prolonged stress response. The insights obtained from this study further advance our understanding of the physiological roles of lncRNAs by interweaving with RNA modifications. With the newly identified lncRNAs on the rise and the growing appreciation of epitranscriptomics, uncovering additional layers of gene regulation would lead to a better understanding of stress response pathways.

Materials and Methods

Cell Lines and Reagents. MEF and HeLa cells were maintained in Dulbecco's Modified Eagle's Medium with 10% fetal bovine serum. Antibodies used in the immunoblotting are as follows: anti-Hsp70/Hsp72 (VWR SPA-810), anti-Hsp105/Hsp110 (Abcam ab109624), anti–β-Actin (Sigma A5441), anti-U1 snRNP70 (Santa Cruz sc-390899), anti-Histone H2B (Cell Signaling Technology 8135), anti-HSF1 (Cell Signaling Technology 4356S), anti-METTL3 (Abcam ab195352), anti-METTL14 (Sigma 038002), anti-YTHDC1 (Cell Signaling Technology 81504S), anti-m^{6}A (Millipore ABE572 and Synaptic Systems 202 003), anti-YTHDF2 (Proteintech 24744-1-AP), anti-H3K9me3 (Epigentek A-4036-025), and anti-H3K27me3 (Abcam ab192985).

Plasmid Constructions. The promoter of mouse *Hspa1a* and *Actb* were amplified by PCR using genomic DNA extracted from MEFs and cloned into Mlu I and Hind III sites of pcDNA3.1-luciferase. For construction of CRISPR-Display plasmids, Bbs I sites were first added to pCMV/3′ Box_(GLuc)_TOP1 (Addgene 68434) by Q5 Site-Directed Mutagenesis Kit (New England Biolabs [NEB] E0554S). Genes encoding *Heat* were amplified by RT-PCR using total RNA extracted from heat-stressed MEFs and subcloned into the resulting pCMV/3′ Box using Gibson assembly (NEB E2611S) to obtain pCMV-*Heat* plasmid. sgRNAs were inserted into Bbs I site of pCMV-*Heat*. To generate pcDNA3.1-APEX2-HSF1, genes encoding *APEX2* were amplified by PCR from pcDNA3.1-APEX2, which was obtained from ref. 36 and subcloned into pcDNA3.1-HSF1 (30) by Gibson assembly. The primers used are in *SI Appendix*, Table S1.

Lentiviral shRNAs. shRNA targeting sequences are in *SI Appendix*, Table S1. All the shRNA targeting sequences were cloned into DECIPHER pRSI9-U6-(sh)-UbiC-TagRFP-2A-Puro (Cellecta). Lenti-X 293T cells (Clontech) were used to package lentiviral particles. The supernatants containing virus were collected and filtered at 48 h after transfection. For infection, the lentivirus was added to MEF cells for 24 h. After selection by 2 mg/mL puromycin, YTHDC1 knockdown MEF cells were collected and characterized.

Cell Fractionation. MEF cells were fractionated according to a previously published procedure (37). Briefly, 1×10^7 cells were centrifuged with 500 *g* to collect the cell pellet and washed with phosphate-buffered saline (PBS) buffer. To lysate the cells, 200 μL ice-cold cytoplasmic lysis buffer (10 mM Tris-HCl pH 7.5, 0.15% Nonidet P-40, 150 mM NaCl, 25 μM α-amanitin, 10 U SUPERase In, and protease inhibitor mix) was added and incubated on ice for 5 min. The cell lysates were gently transferred to 500 μL ice-cold sucrose buffer (25% sucrose, 10 mM Tris-HCl pH 7.5, 0.15% Nonidet P-40, 150 mM NaCl, 25 μM α-amanitin, 10 U SUPERase In, and protease inhibitor mix) and centrifuged at 4 °C with 16,000 *g* for 5 min. The supernatant was collected as cytoplasmic fraction. Then, nuclei pellets were washed by 500 μL ice-cold nuclei wash buffer (0.1% Triton X-100, 1 mM EDTA, in 1× PBS, 25 μM α-amanitin, 10 U SUPERase In, and protease inhibitor mix) followed by centrifugation at 4 °C with 1,150 *g* for 2 min. After removing the supernatant, the nuclei pellet was resuspended in

200 μL ice-cold glycerol buffer (20 mM Tris-HCl pH 8.0, 75 mM NaCl, 0.5 mM EDTA, 0.85 mM dithiotheitol (DTT), 50% glycerol, 10 U SUPERase In, and protease inhibitor mix). The nuclei suspension was mixed with 200 μL nuclei lysis buffer (1% Nonidet P-40, 20 mM Hepes pH 7.5, 300 mM NaCl, 1 M Urea, 0.2 mM EDTA, 1 mM DTT, 25 μM α-amanitin, 10 U SUPERase In, and protease inhibitor mix) for 2 min followed by centrifugation at 4 °C with 18,500 *g* for 2 min to obtain soluble nucleoplasm fraction and insoluble chromatin-associated fraction.

Immunoblotting. Sodium dodecyl sulphate-polyacrylamide gel electrophoresis (SDS-PAGE) gel was used to separate proteins with different mass. Then, proteins were transferred from SDS-PAGE to PVDF membranes (Fisher). Membranes were blocked in blocking buffer containing Tris-buffered saline (TBS), 5% nonfat milk, and 0.1% Tween-20 for 30 min at room temperature with shaking. Primary antibodies were diluted in blocking buffer (1:1,000) and added to membrane overnight at 4 °C. The membrane was washed with Tris-buffered saline with 0.1% Tween 20 (TBST) three times followed by incubation with horseradish peroxidase–coupled secondary antibodies for 1 h at room temperature. The membrane was washed by TBST three times, and immunoblots were visualized using enhanced chemiluminescence (ECL-Plus, GE Healthcare).

mRNA Stability Measurement. Cells were treated with actinomycin D (10 mg/mL) for different times before trypsinization and collection. For different samples, an equal amount of RNA spike-in control was added for normalization. Total RNA was isolated by TRIzol Reagent (Invitrogen). After reverse transcription (see *Real-Time qPCR*), the mRNA levels of transcripts of interest were measured by real-time qPCR.

Real-Time qPCR. The complementary DNA (cDNA) was obtained by reverse transcription using a High Capacity cDNA Reverse Transcription Kit (Invitrogen). Real-time PCR was performed using Power SYBR Green PCR Master Mix (Applied Biosystems) and run on a LightCycler 480 Real-Time PCR System (Roche Applied Science). Primers are listed in *SI Appendix*, Table S1.

Nascent Real-Time qPCR. Nascent RNA was labeled by 1 mM 4-Thiouridine (s4U) for 10 min. Nuclei was extracted immediately as mentioned above (see *Cell Fractionation*), and TRIzol was added to extract nuclear RNA. s4U-labeled nascent RNA was enriched according to a previously published procedure with some modifications (38). Briefly, 5 to 10 μg s4U-labeled nuclear RNA was biotinylated with 5 μg MTSEA biotin-XX (Biotium 90066) in the biotinylation buffer (25 mM Tris pH 7.4, 2.5 mM EDTA) at room temperature for 1.5 h. Unbound MTSEA biotin-XX was removed by equal volume of chloroform/isoamyl alcohol (24:1) (Sigma C0549), and RNA was precipitated for 30 min at 4 °C with 1:10 volume of 5 M NaCl and an equal volume of isopropanol. RNA pellet was obtained by centrifugation at 13,000 rpm for 15 min. After washing with 75% ethanol, the RNA pellet was resuspended in 100 μL RNase-free H_2O. Purified RNA was denatured at 65 °C for 10 min, followed by rapid cooling on ice for 5 min. 4sU-labeled and unlabeled RNA was separated by using Dynabeads M-280 Streptavidin (Invitrogen 11206D). Nascent RNA was eluted with 200 μL 0.1 M DTT and precipitated with 20 μL 3 M NaAc, 2 μL glycogen, and 0.6 mL ice-cold ethanol. Finally, the purified 4sU-labeled nascent RNA was used for reverse transcription and real-time PCR. Primers are specific to exon–intron junction regions of nascent RNAs, which are listed in *SI Appendix*, Table S1.

ASO Knockdown. ASO transfections targeting mouse *Heat* RNA or human *LOC105370148* RNA were conducted using Lipofectamine 2000 Transfection Reagent (Invitrogen 11668-500). In brief, cells were treated with locked nucleic acid (LNA) with a final concentration 50 nM for 6 h before downstream experiments. The LNA sequences are listed in *SI Appendix*, Table S1.

Real-Time Luciferase Assay. Cells grown in 35-mm dishes were transfected with 1 μg plasmid containing the luciferase gene for 6 h. After 1 h heat stress (42 °C), cells were incubated at 37 °C, and 1 mM luciferase substrate D-luciferin (Registech 360223) was added into the culture medium. Luciferase activity was monitored and recorded using Kronos Dio Luminometer (Atto).

CRISPR-Display (Plasmid/RNA). CRISPR-Display experiments were performed according to a previously published procedure (39) with some modifications. For plasmid version, pCMV-dCas9 plasmid and pCMV-sgRNA-Heat plasmid were transfected into cells. After 18 h, cells were subject to heat stress (42 °C, 1 h) and recovery (37 °C) for different times. For RNA version, the pCMV-sgRNA-*Heat* plasmid was used as the templates to generate sgRNA-*Heat* RNA using the MEGAscript T7 Kit (Invitrogen AM1334). To obtain sgRNA-*Heat* with the adenosine replaced with m^6A, in vitro transcription was conducted in a reaction in which 5% of the adenosine was replaced with N^6-methyladenosine. Cells were first transfected with pCMV-dCas9 for 18 h followed by a second transfection with sgRNA-*Heat* or sgRNA-*Heat* (m^6A). After 3 h, cells were subject to heat stress (42 °C, 1 h) and recovery (37 °C) for different times. sgRNA targeting sequences are listed in *SI Appendix*, Table S1.

ChIP. Cells were cross-linked using 1% formaldehyde for 10 min at room temperature, and the reaction was quenched by addition of 250 mM Glycine for 5 min. A total of 500 μL hypotonic buffer (5 mM Hepes pH 8.0, 85 mM KCl, 0.5% Nonidet P-40, and protease inhibitor mix) was added to cell pellets. After centrifugation at 1,000 *g* for 5 min at 4 °C, the supernatant containing cytoplasmic fraction was removed. The chromatin fraction was resuspended in 400 μL radioimmunoprecipitation assay buffer (PBS, 1% Nonidet P-40, 0.1% SDS, 0.5% sodium deoxycholate, and protease inhibitor mix). After 20 min of incubation on ice, chromatin was fractionated by sonication (Bioruptor) for 30 s on and 30 s off for a of total 15 min at the highest setting to achieve a mean DNA fragment size of 200 to 1,000 base pair. After centrifugation for 15 min at 21,000 *g* at 4 °C, the supernatant was collected followed by antibody addition (1: 100 ratio) and rotated overnight. Protein A/G beads were precleared with 100 μg bovine serum albumin and 100 μg sonicated sperm DNA followed by incubation with the lysates for 3 h. The beads were washed in a sequential manner by lysis buffer, high salt buffer (1% TrionX-100, 0.1% sodium deoxycholate, 50 mM Tris-HCl pH 8.0, 0.5 M NaCl, and 5 mM EDTA), LiCl immune complex wash buffer (0.25 M LiCl, 0.5% Nonidet P-40, 0.5% sodium deoxycholate, 10 mM Tris-HCl pH 8.0, and 1mM EDTA), and TE buffer (10 mM Tris-HCl pH 8.0 and 1mM EDTA). Finally, the complex was eluted by 200 μL elution buffer (1% SDS and 0.1 M NaHCO3) at room temperature for 15 min. Then, 10 μL 5M NaCl was added to reverse the cross-link within the antibody–DNA complex at 65 °C for 4 h, followed by addition of 10 μL 0.5M EDTA, 20 μL Tris-HCl pH 8.0, 1 μL proteinase K, and RNase A at 50 °C for 1 h. DNA was purified by phenol/chloroform and chloroform extraction and isopropanol precipitation. The primers used for downstream qPCR are listed in *SI Appendix*, Table S1.

RNA-Binding Protein IP. For zero-distance cross-linking, cells were pretreated with 100 μM s4U for 14 h followed by heat shock stress (42 °C for 1 h and 37 °C for 1 h). Cells were washed with PBS once and irradiated at 0.15 J cm^{-2} total energy of 365 nm ultraviolet light in a Stratalinker 2400. Cells were collected in lysis buffer (20 mM Tris-HCl pH 7.4, 150 mM NaCl, 5 mM $MgCl_2$, 1 mM DTT, 1% Triton X-100, and 40 U/mL RNaseOUT, protease inhibitor mix) followed by sonication (Bioruptor) for 30 s on and 30 s off for 15 min at the highest setting. Lysates were then clarified by centrifugation at 21,000 *g* at 4 °C for 15 min, and the supernatant was collected. HSF1 or YTHDC1 antibodies were added into the lysates for 2 h at 4 °C. IgG agarose beads were then added into the mixture for 3 h, and the beads were washed by lysis buffer three times. Washed beads were treated with 0.1 U μL^{-1} DNase I (ThermoFisher Scientific EN0521) at 37 °C for 30 min and 1 μg μL^{-1} proteinase K (ThermoFisher Scientific AM2548) at 50 °C for 30 min, followed by RNA extraction and RT-qPCR. qPCR primers are listed in *SI Appendix*, Table S1.

Biotin-Phenol Labeling in Live Cells. Biotin-phenol labeling was performed as described before (40). Briefly, genes encoding APEX2 were transfected into MEF cells. After 24 h, cells were incubated with 0.5 mM Biotinyl tyramide (Sigma SML2135) for 30 min at 37 °C. The biotinylation reaction was initiated by the addition of 1 mM H_2O_2 for 1 min. The reaction was stopped with quenching buffer containing 10 mM sodium azide, 10 mM sodium ascorbate, and 5 mM Trolox. Cells were washed three times with ice-cold PBS. For Western blotting, SDS-PAGE loading buffer was added to cell pellets and streptavidin-horseradish peroxidase (HRP) was used to detect biotinylated proteins. For RNA assay, cells were lysated in lysis buffer (50 mM Tris-HCl, pH 7.5, 150 mM NaCl, 0.5% sodium deoxycholate, 1% Triton X-100, 10 mM sodium azide, 10 mM sodium ascorbate, 5 mM Trolox, and 40 U/mL RNaseOUT, protease inhibitor mix) for 15 min on ice. After centrifugation at 13,000 rpm for 10 min at 4 °C, the supernatant was incubated with 100 μL Dynabeads M-280 Streptavidin (Invitrogen 11206D) at 4 °C for 2 h. Beads were then washed with lysis buffer six times, and RNA was extracted by the TRIzol Reagent.

Recombinant Protein Purification. Recombinant eIF4E-GST and His_6-mHSF1 proteins were purified from *E. coli* bacteria BL21 (DE3) (Agilent Technology 200131) transformed by pGEX-6p-1-eIF4E (41) and pET28a-His_6-mHSF1, respectively. To induce protein expression, 0.5 mM IPTG was added at 20 °C for 12 h. For eIF4E purification, cells were lysed in lysis buffer (20 mM Tris-HCl pH 7.5, 300 mM NaCl, 10% glycerol, 5 mM DTT, and 0.5 mM PMSF) and sonicated for 10 min. Cell debris was removed by centrifugation at 15,000 rpm for 30 min.

The supernatant was incubated with 2 mL equilibrated Pierce Glutathione Agarose for 2 h at 4 °C. The resin was washed five times with lysis buffer and used in GST pull-down assay. For mHSF1 purification, cells were lysed in lysis buffer (20 mM Tris-HCl pH 7.5, 300 mM NaCl, 10% glycerol, 5 mM DTT, and 0.5 mM PMSF) containing 10 mM imidazole. After sonication and centrifugation, the supernatant was incubated with 1 mL Ni-NTA Agarose (Qigen 30210) for 1 h at 4 °C. The resin was washed five times with lysis buffer containing 20 mM imidazole, and proteins were eluted in lysis buffer containing 250 mM imidazole. The eluted His_6-mHSF1 was then dialyzed and concentrated in EMSA reaction buffer (10 mM Tris-HCl, pH 7.5, 100 mM NaCl, 10% glycerol, 40 U/mL RNaseOUT) using Amicon Ultra 15 mL Filters (30 kDa; Sigma, UFC9030).

In Vitro Methylation Assay. Fusion proteins of METTL3/METTLM14 (M3/M14) and HSF1 were purified from *E. coli*. The in vitro methylation assay was performed in a 50 μL reaction mixture containing 400 nM in vitro transcribed *Heat* RNA, 20 mM Tris pH 7.5, 50 μM $ZnCl_2$, 1 mM DTT, 0.01% Triton X, 0.2 U/μL RNaseOUT, 1% glycerol, 0.5 μCi (methyl-3H)AdoMet (PerkinElmer), and 200 nM M3/M14, with or without 1 μM HSF1. The mixture was incubated at 30 °C for 1 h and then stopped by adding TRIzol Reagent (Invitrogen). RNA after reaction was precipitated and purified using sodium acetate at −20 °C for at least 2 h. The precipitated RNA was subjected to radioactivity measurement using scintillation counting (Beckman).

Measurement of Exon Skipping. Total RNA was extracted from MEF cells using TRIzol Reagent (Invitrogen). For PCR detecting alternative splicing changes, cDNA was synthesized using SuperScript III Reverse Transcriptase (Thermo Fisher Scientific, 18080044) with Oligo dT primers based on the manufacturer's protocol. PCR reactions were carried out using Taq DNA Polymerase (Genescript, E00101) on a Mastercycler nexus gradient PCR machine (Eppendorf, 2231000765) in 25 μL reaction volume and 35 cycles. The primers used are listed in *SI Appendix*, Table S1.

EMSA. The m^6A-unmodified or -modified *Heat* was synthesized by using MEGAscript T7 Kit (Invitrogen AM1334). FAM-HSE DNA oligonucleotides were synthesized from Integrated DNA Technologies. Forward (5′-6-FAM-AACGAGAATGTTCGCGAAGTTTCTGGCT) and reverse (AGCCAGAAACTTCGCGAACATTCTCGTT) strands were mixed and denatured at 85 °C for 5 min and slowly cooled down to form double stranded DNA. The purified HSF1 and *Heat* or FAM-HSE were incubated on ice for 10 min in binding buffer containing 10 mM Tris-HCl, pH 7.5, 100 mM NaCl, 10% glycerol, and 40 U/mL RNaseOUT. The RNA–protein mixture was loaded on 1% agarose gel and run at 100 V on ice for 20 min. FAM signal was recorded at its corresponding excitation wavelength using a ChemiDoc imaging system (Bio-Rad). *Heat* RNA was detected by staining the gel with ethidium bromide for 10 min.

Polysome Profiling Analysis. Sucrose solutions were made in polysome buffer containing 100 mM KCl, 10 mM Hepes, pH 7.4, 5 mM $MgCl_2$, and 100 mg/mL cycloheximide. A 15 to 45% (weight/volume) sucrose density gradient was prepared in an SW41 μLtracentrifuge tube (Backman) using a Gradient Master (BioComp Instruments). Cells were lysed in polysome lysis buffer (polysome buffer and 2% Triton X-100) followed by centrifugation at 14,000 rpm for 10 min at 4 °C to remove cell debris. Then, 500 μL supernatant was added onto the top of sucrose gradients followed by centrifugation for 2.5 h at 38,000 rpm 4 °C in an SW41 rotor. Samples were fractionated using an automated fractionation system (Isco) that continually monitors OD254 values at 750 μL/min.

RNA-Seq. Total RNA was fragmented with fragmentation buffer (10 mM Tris-HCl, pH 7.0, and 10 mM $ZnCl_2$) at 94 °C for 5 min. To stop the reaction, 50 mM EDTA was added immediately. RNA-seq library construction was performed as described before with changes (42). Briefly, 4 μg fragmented RNA was dephosphorylation in the 15 μL mixture containing 1 × T4 polynucleotide kinase buffer, 10 U SUPERase In, and 20 U T4 polynucleotide kinase at 37 °C for 1 h. RNA was separated on a 15% polyacrylamide TBE-urea gel (Invitrogen). Gels corresponding to 40 to 60 nucleotides (nt) were excised and dissolved in 400 μL RNA elution buffer (300 mM NaOAc, pH 5.5, 1 mM EDTA, and 0.1 U mL^{-1} SUPERase In) overnight. After removal of gel debris using Spin-X column (Corning), RNA was precipitated by one-tenth volumes of 3 M sodium acetate (pH 5.2), 100 μg mL^{-1} glycogen, and 3 volumes of 100% ethanol overnight. RNA pellets were precipitated by centrifuging at 15,000 rpm for 20 min and washed by 75% ethanol. Then, RNA was dissolved in 3 μL nuclease-free H_2O. A total of 1 μL 0.15 μg/μL library construction (LC)-linker (*SI Appendix*, Table S1) was mixed with RNAs at 70 °C for 90 s followed by cooling down to room temperature. Ligation was performed in a 12 μL mixture containing 1× T4 RNL2 reaction buffer, 10 U SUPERase In, 15% PEG8000, and 20 U T4 RNA ligase 2 truncated at 22 °C for 4 h. For reverse transcription reaction, 1 μL 2.5 μM LC-RT primer (*SI Appendix*, Table S1) was added to the ligation products and denatured at 80 °C for 2 min and cooled down on ice for 5 min. The linker ligated RNA was then mixed with 0.5 mM dNTP, 20 mM Tris-HCl pH 8.4, 50 mM KCl, 5 mM $MgCl_2$, 10 mM DTT, 40 U RNaseOUT, and 200 U SuperScript III at 50 °C for 1 h, followed by 70 °C for 3 min. The cDNA was ethanol precipitated and dissolved in 15 μL nuclease-free H_2O. Circularization reaction was performed in a mixture containing 1× CircLigase buffer, 2.5 mM $MnCl_2$, 1 M Betaine, and 100 U CircLigase II (Epicenter) at 60 °C for 1 h. The reaction was heat inactivated at 80 °C for 10 min followed by ethanol precipitation. PCR was performed in a 20 μL mixture containing 1× HF buffer, 0.2 mM dNTP, 0.5 μM PCR primers (LC-PCR-F1/R1, *SI Appendix*, Table S1), and 0.5 U Phusion polymerase. The PCR was initiated at 98 °C for 30s, then 98 °C for 10 s, 65 °C for 20 s, 72 °C for 20 s for 12 cycles. PCR products were separated on a nondenaturing 8% polyacrylamide TBE gel. Expected DNA at 180 bp was excised and soaked by 400 μL DNA elution buffer (300 mM NaOAc, pH 5.5, 1 mM EDTA, 20 U mL^{-1} SUPERase In) overnight. After removal of gel debris using Spin-X column, samples were ethanol precipitated and dissolved in 15 μL nuclease-free H_2O. Finally, samples were sequenced (Illumina HiSeq) by using sequencing primer (LC-Seq-R, *SI Appendix*, Table S1)

m^6A-Seq. For capturing m^6A containing RNAs, 400 μg fragmented RNA was incubated with 5 μg anti-m^6A antibody (Millipore ABE572) and 5 μg anti-m^6A antibody (Synaptic Systems 200 203) in the IP buffer (10 mM Tris-HCl, pH 7.4, 150 mM NaCl, and 0.1% Nonidet P-40) for 2 h at 4 °C. Then Protein A/G beads were added for 2 h at 4 °C. After washing with IP buffer three times, bound RNA was eluted by elution buffer (6.7 mM N^6-mthyladenosine 5′-monophosphate sodium salt in IP buffer), followed by ethanol precipitation. RNA was dissolved in 10 μL nuclease-free H_2O and used for library construction. m^6A-seq library construction was performed as described before with minor changes (35). Briefly, RNA was dephosphorylated (see *RNA-Seq*) and polyA tailed in a 20-μL mixture containing 1× poly(A) polymerase buffer, 1 mM ATP, 0.1 U mL^{-1} SUPERase In, and 3 U *E. coli* poly(A) polymerase at 37 °C for 45 min. For reverse transcription, 1 μL 2.5 μM RT primers (MCA02, LGT03, YAG04, HTC05; *SI Appendix*, Table S1) were added to the ligation products and denatured at 80 °C for 2 min and cooled down on ice for 5 min. Reverse transcription, circularization, and PCR were performed as described above (see *RNA-Seq*). Expected DNA at 140 bp was excised, and DNA was obtained as mentioned above (see *RNA-Seq*). PCR primers (qNTI200 and qNTI201) and sequencing primer (LC-seq-R) are listed in *SI Appendix*, Table S1.

Reads Alignment. Low quality reads and 3′ adaptors were trimmed by Cutadapt (43). For chrRNA-seq and cytRNA-seq, reads were aligned to mm10 using TopHat (44) with the following parameters: –bowtie1–no-novel-juncs. Annotation file was obtained from Ensembl (GRCm38.83). Only unique aligning reads (NH:i:1) were used. PCR duplicates were removed based on unique molecular identifiers (UMI, 4 random nucleotides at the 5′ end of sequencing reads). That is, for the reads with the same length and aligning position, one read was retained arbitrarily; the others with same UMI were removed.

Measurement of Expression Level. For chrRNA-seq and cytRNA-seq, reads per kilo base per million mapped reads (RPKM) was calculated by dividing aligning reads by gene length and sample size. Stress-induced genes were defined as the genes with chrRNA fold change upon heat shock higher than 2.

Calculation of Exon/Intron Ratio. For each gene, reads aligned to exon and intron regions were counted, respectively. For overlapping exons, the most upstream exon was used. To avoid misinterpretations due to insufficient information, genes with exon or intron in length < 1,000 nt or total aligning reads < 100 were excluded.

Statistical Analysis and Graphics. All statistical analyses were performed using the R. Hierarchical clustering was performed by the R function hclust. The heatmap was made by the R package gplots.

Data Availability. Sequencing data have been deposited in Gene Expression Omnibus with the accession GSE173517.

ACKNOWLEDGMENTS. We thank S.B.Q. laboratory members for helpful discussions. We are grateful to Cornell University Life Sciences Core Laboratory Center for sequencing support. This work was supported by US NIH (R01GM1222814 and DP1GM142101) and Howard Hughes Medical Institute Faculty Scholar (55108556) to S.-B.Q.

1. K. Richter, M. Haslbeck, J. Buchner, The heat shock response: Life on the verge of death. *Mol. Cell* **40**, 253–266 (2010).
2. R. Panniers, Translational control during heat shock. *Biochimie* **76**, 737–747 (1994).
3. T. J. McGarry, S. Lindquist, The preferential translation of Drosophila hsp70 mRNA requires sequences in the untranslated leader. *Cell* **42**, 903–911 (1985).
4. R. I. Morimoto, Regulation of the heat shock transcriptional response: Cross talk between a family of heat shock factors, molecular chaperones, and negative regulators. *Genes Dev.* **12**, 3788–3796 (1998).
5. J. Anckar, L. Sistonen, Regulation of HSF1 function in the heat stress response: Implications in aging and disease. *Annu. Rev. Biochem.* **80**, 1089–1115 (2011).
6. J. J. Quinn, H. Y. Chang, Unique features of long non-coding RNA biogenesis and function. *Nat. Rev. Genet.* **17**, 47–62 (2016).
7. S. Djebali *et al*., Landscape of transcription in human cells. *Nature* **489**, 101–108 (2012).
8. M. Guttman, J. L. Rinn, Modular regulatory principles of large non-coding RNAs. *Nature* **482**, 339–346 (2012).
9. H. Wu, L. Yang, L. L. Chen, The diversity of long noncoding RNAs and their generation. *Trends Genet.* **33**, 540–552 (2017).
10. P. Preker *et al*., PROMoter uPstream Transcripts share characteristics with mRNAs and are produced upstream of all three major types of mammalian promoters. *Nucleic Acids Res.* **39**, 7179–7193 (2011).
11. K. W. Vance, C. P. Ponting, Transcriptional regulatory functions of nuclear long noncoding RNAs. *Trends Genet.* **30**, 348–355 (2014).
12. R. F. Place, E. J. Noonan, Non-coding RNAs turn up the heat: An emerging layer of novel regulators in the mammalian heat shock response. *Cell Stress Chaperones* **19**, 159–172 (2014).
13. S. L. Ponicsan, J. F. Kugel, J. A. Goodrich, Genomic gems: SINE RNAs regulate mRNA production. *Curr. Opin. Genet. Dev.* **20**, 149–155 (2010).
14. A. Zovoilis, C. Cifuentes-Rojas, H. P. Chu, A. J. Hernandez, J. T. Lee, Destabilization of B2 RNA by EZH2 activates the stress response. *Cell* **167**, 1788–1802.e13 (2016).
15. I. Shamovsky, M. Ivannikov, E. S. Kandel, D. Gershon, E. Nudler, RNA-mediated response to heat shock in mammalian cells. *Nature* **440**, 556–560 (2006).
16. I. A. Roundtree, M. E. Evans, T. Pan, C. He, Dynamic RNA modifications in gene expression regulation. *Cell* **169**, 1187–1200 (2017).
17. D. P. Patil *et al*., m(6)A RNA methylation promotes XIST-mediated transcriptional repression. *Nature* **537**, 369–373 (2016).
18. J. Liu *et al*., N^6-methyladenosine of chromosome-associated regulatory RNA regulates chromatin state and transcription. *Science* **367**, 580–586 (2020).
19. D. B. Mahat, H. H. Salamanca, F. M. Duarte, C. G. Danko, J. T. Lis, Mammalian heat shock response and mechanisms underlying its genome-wide transcriptional regulation. *Mol. Cell* **62**, 63–78 (2016).
20. A. Mayer *et al*., Native elongating transcript sequencing reveals human transcriptional activity at nucleotide resolution. *Cell* **161**, 541–554 (2015).
21. M. L. Mendillo *et al*., HSF1 drives a transcriptional program distinct from heat shock to support highly malignant human cancers. *Cell* **150**, 549–562 (2012).
22. V. Hung *et al*., Spatially resolved proteomic mapping in living cells with the engineered peroxidase APEX2. *Nat. Protoc.* **11**, 456–475 (2016).
23. S. Geisler, J. Coller, RNA in unexpected places: Long non-coding RNA functions in diverse cellular contexts. *Nat. Rev. Mol. Cell Biol.* **14**, 699–712 (2013).
24. B. Slobodin *et al*., Transcription impacts the efficiency of mRNA translation via Co-transcriptional N6-adenosine methylation. *Cell* **169**, 326–337.e12 (2017).
25. I. A. Roundtree *et al*., YTHDC1 mediates nuclear export of N^6-methyladenosine methylated mRNAs. *eLife* **6**, e31311 (2017).
26. G. Zander *et al*., mRNA quality control is bypassed for immediate export of stress-responsive transcripts. *Nature* **540**, 593–596 (2016).
27. W. Xiao *et al*., Nuclear m(6)A reader YTHDC1 regulates mRNA splicing. *Mol. Cell* **61**, 507–519 (2016).
28. M. J. Cowley *et al*., PINA v2.0: Mining interactome modules. *Nucleic Acids Res.* **40**, D862–D865 (2012).
29. J. H. Feder, J. M. Rossi, J. Solomon, N. Solomon, S. Lindquist, The consequences of expressing hsp70 in Drosophila cells at normal temperatures. *Genes Dev.* **6**, 1402–1413 (1992).
30. S. B. Qian, H. McDonough, F. Boellmann, D. M. Cyr, C. Patterson, CHIP-mediated stress recovery by sequential ubiquitination of substrates and Hsp70. *Nature* **440**, 551–555 (2006).
31. J. A. West *et al*., The long noncoding RNAs NEAT1 and MALAT1 bind active chromatin sites. *Mol. Cell* **55**, 791–802 (2014).
32. V. B. O'Leary *et al*., PARTICLE, a triplex-forming long ncRNA, regulates locus-specific methylation in response to low-dose irradiation. *Cell Rep.* **11**, 474–485 (2015).
33. T. Mondal *et al*., MEG3 long noncoding RNA regulates the TGF-β pathway genes through formation of RNA-DNA triplex structures. *Nat. Commun.* **6**, 7743 (2015).
34. A. Vihervaara *et al*., Transcriptional response to stress is pre-wired by promoter and enhancer architecture. *Nat. Commun.* **8**, 255 (2017).
35. J. Zhou *et al*., Dynamic m(6)A mRNA methylation directs translational control of heat shock response. *Nature* **526**, 591–594 (2015).
36. M. Xue *et al*., Optimizing the fragment complementation of APEX2 for detection of specific protein-protein interactions in live cells. *Sci. Rep.* **7**, 12039 (2017).
37. A. Mayer, L. S. Churchman, Genome-wide profiling of RNA polymerase transcription at nucleotide resolution in human cells with native elongating transcript sequencing. *Nat. Protoc.* **11**, 813–833 (2016).
38. G. Fuchs *et al*., Simultaneous measurement of genome-wide transcription elongation speeds and rates of RNA polymerase II transition into active elongation with 4sUDRB-seq. *Nat. Protoc.* **10**, 605–618 (2015).
39. D. M. Shechner, E. Hacisuleyman, S. T. Younger, J. L. Rinn, Multiplexable, locus-specific targeting of long RNAs with CRISPR-Display. *Nat. Methods* **12**, 664–670 (2015).
40. F. M. Fazal *et al*., Atlas of subcellular RNA localization revealed by APEX-seq. *Cell* **178**, 473–490.e26 (2019).
41. R. A. Coots *et al*., m(6)A Facilitates eIF4F-Independent mRNA Translation. *Mol. Cell* **68**, 504–514.e7 (2017).
42. Y. Mao *et al*., m^6A in mRNA coding regions promotes translation via the RNA helicase-containing YTHDC2. *Nat. Commun.* **10**, 5332 (2019).
43. M. Martin, Cutadapt removes adapter sequences from high-throughput sequencing reads. *EMBnet. J.* **17**, 10–12 (2011).
44. C. Trapnell, L. Pachter, S. L. Salzberg, TopHat: Discovering splice junctions with RNA-seq. *Bioinformatics* **25**, 1105–1111 (2009).